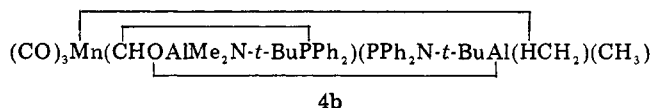
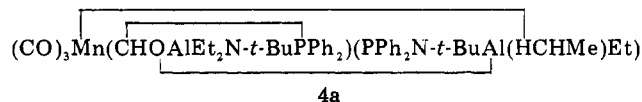


to stand; over a period of hours it gradually turned orange and residual solid slowly dissolved. After 3 days the golden orange solution was filtered and evaporated to a yellow solid (**4b**):  $^1\text{H}$



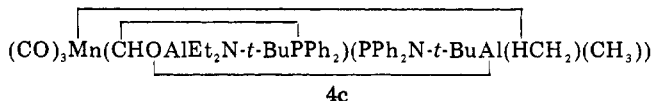
NMR  $\delta$  7.9 (m), 7.3 (m), 7.0 (m,  $\text{C}_6\text{H}_6$ ), 5.17 (dd,  $J = 4.7, 11.1$  Hz,  $\text{MnCHOAlNP}$ ), 1.22 (s), 1.01 (s,  $\text{C}(\text{CH}_3)_3$ ), 0.18 (s), 0.04 (s), -0.01 (s), -1.75 (s,  $\text{Al}(\text{CH}_3)_2$ );  $^{31}\text{P}$  NMR  $\delta$  41.6 (d), 72.1 (d,  $J_{\text{PP}} = 24$  Hz); IR (Nujol)  $\nu_{\text{CO}}$  2000 (s), 1910 (vs)  $\text{cm}^{-1}$ .

**4a.**  $\text{HMn}(\text{CO})_5$  (0.09 g, 0.44 mmol) was added to a solution of **1a** (0.3 g, 0.88 mmol) in 0.5 mL of  $\text{C}_6\text{D}_6$  and the progress of the reaction followed by  $^1\text{H}$  NMR spectroscopy. After 20 min all  $\text{HMn}(\text{CO})_5$  had been consumed and **2a** was the major species present; after 20 h the latter had completely disappeared and had been replaced by **4a**:  $^1\text{H}$  NMR  $\delta$  7.9-7.2 (m,  $\text{C}_6\text{H}_6$ ), 5.5 (dd,  $J =$



5.5, 10.0 Hz,  $\text{MnCHOAlNP}$ ), 1.2 (s), 1.0 (s,  $\text{C}(\text{CH}_3)_3$ ), -0.6 (m,  $\text{AlCH}_2\text{CH}_3$ ) (the remaining  $\text{AlEt}$  signals overlapped and could not be fully resolved);  $^{31}\text{P}$  NMR  $\delta$  41.1 (d), 70.9 (d,  $J_{\text{PP}} = 22$  Hz); IR (Nujol)  $\nu_{\text{CO}}$  1992 (s), 1968 (w), 1908 (s)  $\text{cm}^{-1}$ . The same product was obtained on the addition of 1 equiv of **1a** to a solution of **2a**.

**4c.** A solution of  $\text{HMn}(\text{CO})_5$  (0.06 g, 0.29 mmol) and **1a** (0.1 g, 0.29 mmol) in  $\text{C}_6\text{D}_6$  was allowed to react for 4 h and then treated with **1b** (0.09 g, 0.29 mmol). After 15 min the NMR showed nearly complete conversion to **4c**:  $^1\text{H}$  NMR  $\delta$  7.9-7.2 (m,  $\text{C}_6\text{H}_6$ ), 5.2 (dd,



$J = 5.3, 11.2$  Hz,  $\text{MnCHOAlNP}$ ), 1.2 (s), 1.0 (s,  $\text{C}(\text{CH}_3)_3$ ), -0.07 (s), -1.9 (s,  $\text{AlCH}_3$ ) ( $\text{AlEt}$  signals were partly obscured by  $\text{C}(\text{CH}_3)_3$  peaks); IR (cyclohexane)  $\nu_{\text{CO}}$  1997 (s), 1965 (w), 1910 (s)  $\text{cm}^{-1}$ .

$(\text{CO})_3(\text{P}(\text{OPh})_3)\text{Mn}(\text{CHOAlEt}_2\text{N-}t\text{-BuPPPh}_2)$  (**5**). A solution of **2a**, prepared as in the preceding reaction, was treated with 1 equiv of  $\text{P}(\text{OPh})_3$ . Over 30 min the color faded to light orange, accompanied by gas evolution, and the NMR showed complete conversion of **2a**:  $^1\text{H}$  NMR  $\delta$  7.9-7.2 (m,  $\text{C}_6\text{H}_6$ ), 4.7 (dd,  $J = 11, 27.5$  Hz,  $\text{MnCHOAlNP}$ ), 1.2 (s,  $\text{C}(\text{CH}_3)_3$ ), 0.5 (m,

$\text{AlCH}_2\text{CH}_3$ ) (the  $\text{AlCH}_2\text{CH}_3$  signal was obscured by the  $\text{C}(\text{CH}_3)_3$  resonance);  $^{31}\text{P}$  NMR 36.2 (d), 128.3 (d,  $J_{\text{PP}} = 12$  Hz); IR (cyclohexane)  $\nu_{\text{CO}}$  1990 (s), 1960 (s), 1895 (s)  $\text{cm}^{-1}$ . The same product was generated by adding **1a** to  $\text{HMn}(\text{CO})_4(\text{P}(\text{OPh})_3)$ .

**CpMo(CO) $_3$ AlMe $_2$ N- $t$ -BuPPPh $_2$ H** (**15**). A solution of  $\text{CpMo}(\text{CO})_3\text{H}$  (0.32 mmol) and **1b** (0.32 mmol) in  $\text{C}_6\text{D}_6$  (0.5 mL) was allowed to react while monitoring the  $^1\text{H}$  NMR spectrum. After several hours, the resonances due to starting materials had been completely replaced by those assigned to product. (The latter gradually broadened and decayed on further standing.) Several milliliters of hexane were added, and the mixture was cooled overnight at -40  $^\circ\text{C}$ ; a brownish, oily material separated out and was dried in vacuo. Attempts at crystallization were unsuccessful:  $^1\text{H}$  NMR  $\delta$  7.8 (d,  $J_{\text{PH}} = 500$  Hz,  $\text{HPPPh}_2$ ), 7.6 (m), 7.2 (m,  $\text{C}_6\text{H}_6$ ), 5.27 (s, Cp), 1.2 (s,  $\text{C}(\text{CH}_3)_3$ ), -0.4 (s,  $\text{AlCH}_3$ );  $^{31}\text{P}$  NMR  $\delta$  13.6 (d (with no  $^1\text{H}$  decoupling, this signal appeared as a doublet ( $J \approx 500$  Hz) of multiplets; with the decoupler on, it collapsed to a doublet of about 15 Hz splitting; not enough power was available to completely remove the large P-H coupling); IR ( $\text{C}_6\text{H}_6$ )  $\nu_{\text{CO}}$  1930 (s), 1845 (s), 1570 (m, br)  $\text{cm}^{-1}$ .

The reaction of  $\text{CpW}(\text{CO})_3\text{H}$  with **1b** proceeded in much the same manner, to give a product with virtually identical spectral parameters. In contrast, the reactions of  $\text{CpM}(\text{CO})_3\text{H}$  ( $M = \text{Cr, Mo, W}$ ) with **1a** were complete within 15 min; although similar NMR peaks developed, the products appeared to form much less cleanly; and decomposition as evidenced by NMR peak degradation was significant after only 1 h.

**Structure Determination for 4b.** Small prismatic crystals of **4b** were obtained by dissolving a sample in the minimum amount of benzene, adding hexane until clouding was observed, and storing at -40  $^\circ\text{C}$  for several weeks. The structure was determined by Molecular Structures Corp., College Station, TX. Experimental details and crystal data are summarized in Table VI. Atom positions and key bond parameters are given in Tables II-IV, other data are available as supplementary material.

**Acknowledgment.** We thank C. Schramm and V. Parziale for assistance with NMR studies.

**Registry No.** **1a**, 5573-37-5; **1b**, 83585-38-0; **2a**, 83632-48-8; **2a-d $_1$** , 86480-65-1; **3**, 83585-42-6; **4a**, 83632-49-9; **4b**, 83632-50-2; **4c**, 86480-66-2; **5**, 83649-33-6; **1s**, 86497-03-2;  $\text{HMn}(\text{CO})_5$ , 16972-33-1;  $\text{CpMo}(\text{CO})_3\text{H}$ , 12176-06-6.

**Supplementary Material Available:** Listings of calculated hydrogen positions (Table VII), thermal parameters (Table VIII), torsional angles (Table IX), intermolecular contacts (Table X), least-squares planes (Table XI), and observed and calculated structure factors (Table XII) for complex **4b** (35 pages). Ordering information is given on any current masthead page.

## Formation, Decay, and Spectral Characterization of Some Alkyl- and Aryl-Substituted Carbon-, Silicon-, Germanium-, and Tin-Centered Radicals<sup>1</sup>

C. Chatgillaloglu,<sup>2a</sup> K. U. Ingold,\* J. Luszyk,<sup>2b</sup> A. S. Nazran,<sup>2b</sup> and J. C. Scaiano

Division of Chemistry, National Research Council of Canada, Ottawa, Ontario, K1A 0R6 Canada

Received April 8, 1983

*tert*-Butoxyl abstracts hydrogen from M-H bonds ( $M = \text{Si, Ge, Sn}$ ) with rate constants (300 K) of  $(0.6-2) \times 10^7$  ( $M = \text{Si}$ ),  $\sim 9 \times 10^7$  ( $M = \text{Ge}$ ), and  $(2-4) \times 10^8 \text{ M}^{-1} \text{ s}^{-1}$  ( $M = \text{Sn}$ ), respectively. The radicals  $(\text{alkyl})_3\text{M}\cdot$  show a strong absorption band at  $\lambda < 300$  nm and a weaker band/shoulder at longer  $\lambda$  that shifts from 320 ( $M = \text{C}$ ) to 390 nm ( $M = \text{Sn}$ ). The spectra of  $\text{Ph}_3\text{M}$  show little sensitivity to the heteroatom. Arylsilyl radicals add readily to their precursors; for example,  $\text{Ph}_3\text{Si}\cdot$  adds to  $\text{Ph}_3\text{SiH}$  with  $k_4 = (2.1 \times 0.4) \times 10^5 \text{ M}^{-1} \text{ s}^{-1}$  at 300 K.

We have recently reported kinetic studies by laser flash photolysis on the reactions of triethylsilyl radicals with a

wide variety of substrates,<sup>3-6</sup> on the reactions of *tert*-butoxyl radicals and triplet ketones with silanes,<sup>7</sup> and on

the reactions of alkyl radicals with tri-*n*-butyltin hydride.<sup>8</sup> During this work we became aware that spectral data on group 4 centered radicals (other than the carbon-centered species) are almost completely absent from the literature. Furthermore, there is only limited information on the rates of H atom abstraction from the group 4 heteroatom-hydrogen bonds even by such a commonly employed H atom abstracting radical as *tert*-butoxyl. In the present work we provide spectral and kinetic data to alleviate these deficiencies.

### Experimental Section

**Materials.** Tri-*n*-butylgermanium hydride was kindly provided by Drs. P. J. Stang and M. R. White. All other materials were commercially available and were purified by standard techniques before use. Special care was taken to prevent their autoxidation during storage and handling.

**Procedures.** Most laser flash photolysis experiments were carried out by using the pulses (337.1 nm, ~8 ns, up to 10 mJ/pulse) from a Moletron UV-24 nitrogen laser for excitation. Our computerized system has been described in detail elsewhere.<sup>9</sup> All experiments were carried out on deaerated samples. Two kinetic procedures were employed: (A) For those product radicals ( $R_3M\cdot$  in reaction 1) that showed strong absorptions, the time profile of their formation was monitored at a number of different concentrations of the parent molecule  $R_3MH$ . (B) For those



product radicals that showed only weak absorptions diphenylmethanol was employed as a "probe". We have used this technique, in which the readily detected  $Ph_2\dot{C}OH$  radical formed in reaction 2 is monitored, quite extensively.<sup>7,10</sup> Both techniques



have been used and discussed in earlier papers.<sup>3-10</sup> Both yield absolute rate constants but do not distinguish between sites or modes of attack; i.e., the rate constants include all modes of interaction of  $R_3MH$  with  $Me_3CO\cdot$ . Assignment of the rate constant to a given path such as reaction 1 must be based on chemical knowledge from other techniques, e.g., product analysis or EPR spectroscopy. In both techniques the *tert*-butoxyl radicals were generated by direct photodecomposition of di-*tert*-butyl peroxide.

Transient spectra were obtained by monitoring optical density after reaction 1 was at least 90% complete, the substrate concentration being chosen so that this time was ca.  $\leq 1 \mu s$ . Optical densities could not be measured between ca. 332 and 344 nm because this was too close to the nitrogen laser wavelength of 337 nm. For some radicals the transient spectra were therefore also recorded by using the 308-nm pulses from an excimer laser for excitation. No unusual features were observed in the 332-344-nm range for any of the radicals examined, viz.,  $Ph_3Si\cdot$ ,  $Ph_3Ge\cdot$ , and  $Ph_3Sn\cdot$ . The excimer laser was also used to generate the *tert*-butyl radical by photodecomposition of di-*tert*-butyl ketone.

### Results and Discussion

**Kinetics of Reaction with *tert*-Butoxyl.** Rate constants for reaction 1 at 300 K are summarized in Table I,

Table I. Absolute Rate Data for the Reactions of *tert*-Butoxyl with Several Substrates at 300 K

substrate	method <sup>a</sup>	$k_1,^b M^{-1} s^{-1}$
(alkyl) <sub>3</sub> CH	C	$2.7 \times 10^5$ <sup>c</sup>
PhCH <sub>3</sub>	B	$2.3 \times 10^5$ <sup>d</sup>
Ph <sub>2</sub> CH <sub>2</sub>	B	$(1.3 \pm 0.1) \times 10^6$
Ph <sub>2</sub> CH	A	$(2.6 \pm 0.8) \times 10^6$
Et <sub>3</sub> SiH	B	$(5.7 \pm 0.6) \times 10^6$ <sup>e</sup>
PhSiH <sub>3</sub>	B	$(7.5 \pm 1.3) \times 10^6$ <sup>e</sup>
Ph <sub>2</sub> SiH <sub>2</sub>	A	$(2.0 \pm 0.3) \times 10^7$
Ph <sub>2</sub> SiH	B	$(1.3 \pm 0.1) \times 10^7$
Ph <sub>3</sub> SiH	A	$(7.7 \pm 0.8) \times 10^6$
Ph <sub>3</sub> SiH	B	$(1.1 \pm 0.1) \times 10^7$
Bu <sub>3</sub> GeH	A	$(9.2 \pm 1.4) \times 10^7$
Bu <sub>3</sub> GeH	B	$(8.0 \pm 0.6) \times 10^7$
Ph <sub>3</sub> GeH	A	$(9.2 \pm 0.4) \times 10^7$
Ph <sub>3</sub> GeH	B	$(8.9 \pm 1.7) \times 10^7$
Bu <sub>3</sub> SnH	A	$1.9 \times 10^8$ <sup>f</sup>
Bu <sub>3</sub> SnH	B	$2.2 \times 10^8$ <sup>f</sup>
Ph <sub>3</sub> SnH	A	$(4.3 \pm 0.6) \times 10^8$
Ph <sub>3</sub> SnH	B	$(4.0 \pm 0.5) \times 10^8$

<sup>a</sup> A: direct detection of product radical in di-*tert*-butyl peroxide-isooctane, 1:4 (v/v); for Bu<sub>3</sub>GeH and Bu<sub>3</sub>SnH the rates have been measured in di-*tert*-butyl peroxide. B: detection of product radical via probe technique in di-*tert*-butyl peroxide-benzene, 2:1 v/v. C: competitive methods. <sup>b</sup> Errors reported as  $\pm 2\sigma$  include only random errors. <sup>c</sup> See footnote 25 of ref 3. <sup>d</sup> Reference 10. <sup>e</sup> Reference 7. <sup>f</sup> Reference 36.

Table II. Rate Data for the Decay of  $R_3M\cdot$  Radicals in 1:4 (v/v) Di-*tert*-butyl Peroxide-Isooctane at 300 K

radical	$10^{-6}k_d,$ $M^{-1} s^{-1}$	$2k_3/\epsilon\lambda,$ $cm^{-1} s^{-1}$	$\lambda,$ nm
Et <sub>3</sub> Si·		$1.1 \times 10^7$	308
PhSiH <sub>2</sub>	$(1.5 \pm 0.3)$		
Ph <sub>2</sub> SiH	$(2.1 \pm 0.4)$		
Ph <sub>3</sub> Si·	$(0.21 \pm 0.04)$		
Bu <sub>3</sub> Ge· <sup>a</sup>		$4.2 \times 10^6$	346
Bu <sub>3</sub> Sn· <sup>a</sup>		$3.3 \times 10^6$	400
Ph <sub>3</sub> Sn· <sup>a</sup>		$4.8 \times 10^5$	325

<sup>a</sup> Di-*tert*-butyl peroxide as solvent.

together with a few relevant measurements taken from earlier work. Full kinetic data are available as supplementary material. These rate constants show no unexpected features since H atom abstraction by *tert*-butoxyl, even from alkanes, is a rapid process that is believed to have a rather "early" transition state.<sup>11</sup> Thus, values of  $k_1$  increase as  $R_3M-H$  bond strengths decrease along the series  $M = C < Si < Ge < Sn$ , and indeed with  $Ph_3PbH$  the rate would probably approach diffusion control. Phenyl substitution, even multiple phenyl substitution, has only a small effect on  $k_1$  except in the case of  $M = C$ .<sup>12</sup> In earlier studies involving hydrogen abstraction from silanes,<sup>7</sup> we attributed this similarity to ineffective resonance stabilization of a silicon-centered radical by neighboring phenyl groups, a phenomenon that can be attributed to the larger size of silicon (compared to carbon) and to the pyramidal nature of the radical center. The same arguments apply to the germanes and stannanes, but, in addition, the faster rates can be expected to reduce reaction selectivity.

(11) See, e.g.: Zavitsas, A. A.; Pinto, J. A. *J. Am. Chem. Soc.* **1972**, *94*, 7390-7396 and references cited.

(12) For a discussion as to the reasons for the similarity in the reactivity toward *tert*-butoxyl of toluene and alkanes, see ref 11 and references cited. However, it should be noted that the  $CH_3$  group in toluene is about 9 times more reactive than one of the  $CH_3$  groups in 2,3-dimethylbutane.<sup>13</sup>

(13) Walling, C.; Mintz, M. J. *J. Am. Chem. Soc.* **1967**, *89*, 1515-1519.

(1) Issued as N.R.C.C. No. 22505.

(2) N.R.C.C. Research Associate: (a) 1979-1982; (b) 1982-1983.

(3) Chatgililoglu, C.; Ingold, K. U.; Scaiano, J. C.; Woynar, H. *J. Am. Chem. Soc.* **1981**, *103*, 3231-3232.

(4) Chatgililoglu, C.; Ingold, K. U.; Scaiano, J. C. *J. Am. Chem. Soc.* **1982**, *104*, 5119-5123.

(5) Chatgililoglu, C.; Ingold, K. U.; Scaiano, J. C. *J. Am. Chem. Soc.* **1982**, *104*, 5123-5127.

(6) Chatgililoglu, C.; Ingold, K. U.; Scaiano, J. C. *J. Am. Chem. Soc.* **1983**, *105*, 3292-3296.

(7) Chatgililoglu, C.; Scaiano, J. C.; Ingold, K. U. *Organometallics* **1982**, *1*, 466-469.

(8) Chatgililoglu, C.; Ingold, K. U.; Scaiano, J. C. *J. Am. Chem. Soc.* **1981**, *103*, 7739-7742.

(9) Scaiano, J. C. *J. Am. Chem. Soc.* **1980**, *102*, 7747-7753.

(10) Paul, H.; Small, R. D., Jr.; Scaiano, J. C. *J. Am. Chem. Soc.* **1978**, *100*, 4520-4527.

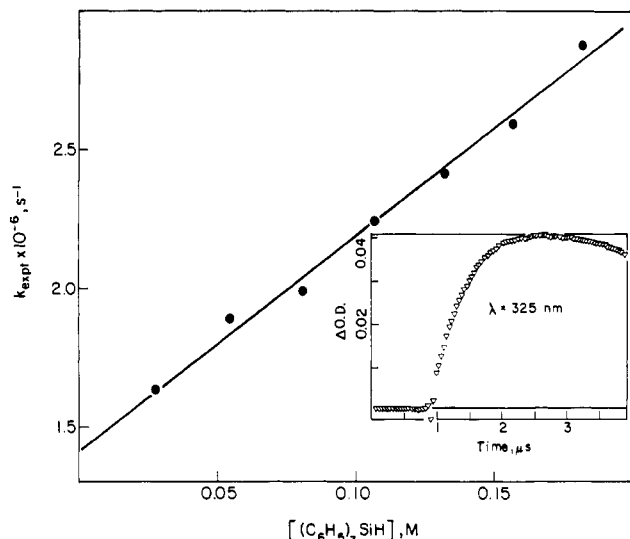
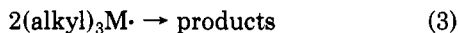


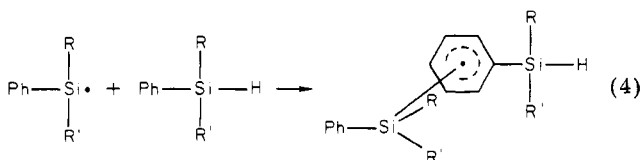
**Figure 1.** Effect of  $\text{Ph}_3\text{SiH}$  on the lifetime of the  $\text{Ph}_3\text{Si}\cdot$  radical in 1:4 di-*tert*-butyl peroxide–isooctane at 300 K. Insert: representative buildup trace for  $[\text{Ph}_3\text{SiH}] = 0.182 \text{ M}$ .

**Decay of Heteroatom-Centered Radicals.** All trialkyl-substituted radicals decayed with “clean” second-order kinetics when generated in di-*tert*-butyl peroxide as solvent (reaction 3). This was expected on the basis of



earlier kinetic EPR studies which have shown that such reactions are diffusion-controlled processes.<sup>14–20</sup> Values of  $2k_3/\epsilon_\lambda$ , where  $\epsilon_\lambda$  is the extinction coefficient at the monitoring wavelength, are given in Table II.

In sharp contrast to the trialkyl substituted radicals, all of the phenyl-substituted silyl radicals decayed with first-order kinetics when generated under similar conditions. The experimental first-order rate constants for radical decay,  $k_{\text{decay}}$ , were linearly dependent on the concentration of the silane precursor. Figure 1 shows, for triphenylsilane as substrate, a representative plot of  $k_{\text{decay}}$  vs.  $[\text{Ph}_3\text{SiH}]$ , as well as (insert) a representative build-up trace. The observed kinetics can be attributed to the addition of the silyl radical to an aromatic ring of the substrate (reaction 4). Such reactions are now well doc-



umented.<sup>6,21–25</sup> The slope of the line in Figure 1 yields  $k_4 = (2.1 \pm 0.4) \times 10^6 \text{ M}^{-1} \text{ s}^{-1}$  for  $\text{Ph}_3\text{Si}\cdot$  addition to  $\text{Ph}_3\text{SiH}$ .

(14) Frangopol, P. T.; Ingold, K. U. *J. Organomet. Chem.* **1970**, *25*, C9–C12.

(15) Watts, G. B.; Ingold, K. U. *J. Am. Chem. Soc.* **1972**, *94*, 491–494.

(16) Gaspar, P. P.; Haizlip, A. D.; Choo, K. Y. *J. Am. Chem. Soc.* **1972**, *94*, 9032–9037.

(17) Hamilton, E. J., Jr.; Fischer, H. *J. Phys. Chem.* **1973**, *77*, 722–724.

(18) Griller, D.; Ingold, K. U. *Int. J. Chem. Kinet.* **1974**, *6*, 453–456.

(19) Schuh, H.-H.; Fischer, H. *Int. J. Chem. Kinet.* **1976**, *8*, 341–356; *Helv. Chim. Acta* **1978**, *61*, 2130–2164.

(20) Huggenberger, C.; Fischer, H. *Helv. Chim. Acta* **1981**, *64*, 338–353.

(21) Eaborn, C.; Jackson, R. A.; Pearce, R. *Chem. Commun.* **1967**, 920.

(22) Sakurai, H.; Hosomi, A. *J. Am. Chem. Soc.* **1971**, *93*, 1709–1714.

(23) Sakurai, H.; Nozue, I.; Hosomi, A. *Chem. Lett.* **1976**, 129–134.

(24) Sakurai, H.; Umino, H.; Sugiyama, H. *J. Am. Chem. Soc.* **1980**, *102*, 6837–6840.

(25) Griller, D.; Marriott, P. R.; Nonhebel, D. C.; Perkins, M. J.; Wong, P. C. *J. Am. Chem. Soc.* **1981**, *103*, 7761–7763.

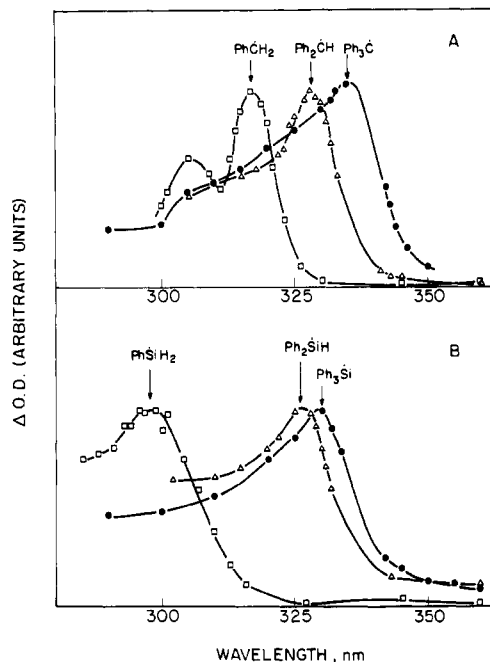


**Figure 2.** Transient spectra for  $\text{PhMH}_2$ ,  $\text{Ph}_2\text{MH}$ , and  $\text{Ph}_3\text{M}\cdot$  radicals ( $\text{M} = \text{C}$  in A and  $\text{M} = \text{Si}$  in B) in 1:4 di-*tert*-butyl peroxide–isooctane at 300 K, typically obtained by using  $\sim 0.05 \text{ M}$  substrate. The continuous traces are simply “artist fits”.

For comparison, the rate constant for  $\text{EtSi}\cdot$  addition to benzene has a value of  $(4.6 \pm 1.0) \times 10^5 \text{ M}^{-1} \text{ s}^{-1}$  at the same temperature.<sup>6,25</sup> Similar experiments with mono- and diphenylsilane yielded  $k_4$  values that were about 1 order of magnitude larger than the values found for the  $\text{Ph}_3\text{Si}\cdot/\text{Ph}_3\text{SiH}$  and  $\text{Et}_3\text{Si}\cdot/\text{C}_6\text{H}_6$  reactions (see Table II and supplementary material). We conclude that silicon substitution activates an aromatic ring toward the addition of a silicon-centered radical and, furthermore, that steric effects in polyphenyl-substituted silyl radicals cause a reduction in their rate of addition to aromatic rings.<sup>26</sup>

In contrast to phenylsilyl radicals, the triphenyltin radical decayed with clean second-order kinetics, suggesting that its addition to an aromatic ring is a relatively slow process.

The decay of  $\text{Ph}_3\text{Ge}\cdot$  approached first-order kinetics, though it systematically showed some deviations, probably as a result of underlying second-order processes. Typical lifetimes for solutions in the 1–10 mM range of  $\text{Ph}_3\text{GeH}$  were around 10–15  $\mu\text{s}$ . Solubility problems frustrated any detailed studies of the potential addition of  $\text{Ph}_3\text{Ge}\cdot$  to the aromatic rings in the precursor.

**Absorption Spectra of Group 4 Centered Radicals.** Mono-, di-, and triphenylsilyl radicals are all blue-shifted with respect to the corresponding carbon-centered radicals (see Figure 2). The magnitude of this blue shift is much greater for  $\text{PhSiH}_2\cdot$  vs.  $\text{Ph}\dot{\text{C}}\text{H}_2$  than for  $\text{Ph}_2\text{SiH}\cdot$  vs.  $\text{Ph}_2\dot{\text{C}}\text{H}$  or  $\text{Ph}_3\text{Si}\cdot$  vs.  $\text{Ph}_3\dot{\text{C}}$ . We tentatively suggest that diphenyl and triphenylsilyl radicals are more nearly planar than the phenylsilyl radical and are thus more nearly equivalent in structure to their carbon-centered radical counterparts than are  $\text{PhSiH}_2\cdot$  and  $\text{Ph}\dot{\text{C}}\text{H}_2$ . Nevertheless, it is highly unlikely that either  $\text{Ph}_2\text{SiH}\cdot$ <sup>27</sup> or  $\text{Ph}_3\text{Si}\cdot$ <sup>30</sup> are actually pla-

(26) The importance of steric factors in reducing the rate of this class of reactions has been previously demonstrated.<sup>23</sup>

(27) For example, a structurally related chiral silyl radical can be generated from 1-naphthylphenylmethylsilane that will react with  $\text{CCl}_4$  to give optically active products with retained stereochemistry.<sup>28,29</sup>

(28) Sakurai, H.; Murakami, M.; Kumada, M. *J. Am. Chem. Soc.* **1969**, *91*, 519–520.

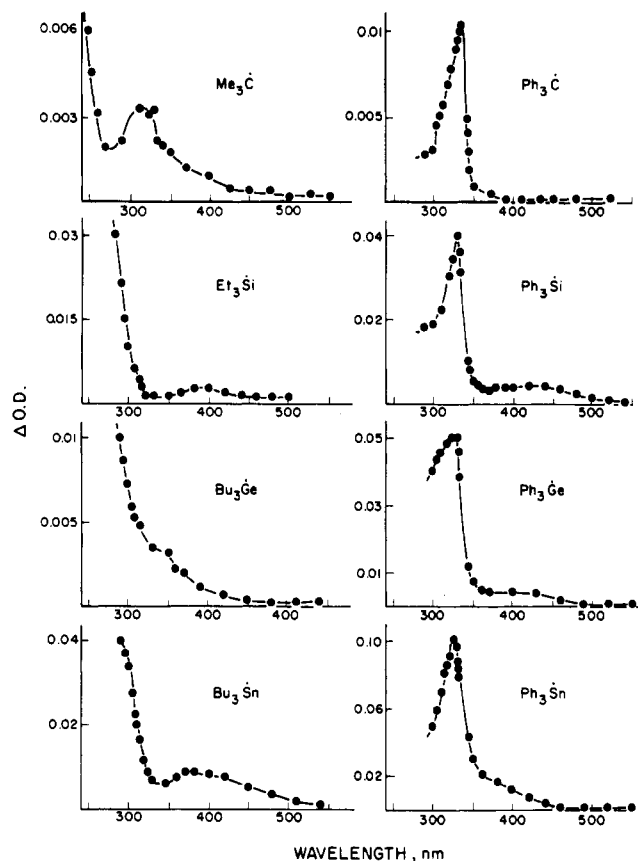


Figure 3. Spectra of several  $R_3M\cdot$  radicals under the same conditions as in Figure 2.

nar.

The absorption spectra of  $(\text{alkyl})_3M\cdot$  and  $\text{Ph}_3M\cdot$  radicals are shown in Figure 3 for  $M = \text{C}, \text{Si}, \text{Ge},$  and  $\text{Sn}$ . These spectra agree with reported data for those radicals, viz.,  $\text{Me}_3\text{C}\cdot$ ,<sup>20,34</sup>  $\text{Ph}_3\text{C}\cdot$ ,<sup>35</sup>  $\text{Et}_3\text{Si}\cdot$ ,<sup>3,7</sup> and  $n\text{-Bu}_3\text{Sn}\cdot$ ,<sup>36</sup> for which all

or part of the spectrum has been published. All  $(\text{alkyl})_3M\cdot$  radicals show a very strong band at  $\lambda < 300$  nm and a weaker band/shoulder at longer wavelengths. The latter shifts to longer wavelengths as the size of  $M$  increases, from about 320 nm for  $\text{Me}_3\text{C}\cdot$  to about 390 nm for  $n\text{-Bu}_3\text{Sn}\cdot$ . Rather surprisingly the  $\text{Ph}_3M\cdot$  radicals show, by contrast, little sensitivity to the heteroatom, there being only a very small blue shift as  $M$  increases in size. In these radicals also there generally appears to be a weak band/shoulder at longer wavelengths. The precise electronic transitions that produce the spectra shown in Figures 2 and 3 are unknown. However, the remarkable similarity between the spectrum of the planar  $\text{Ph}_3\text{C}\cdot$  radical and the spectra of the nonplanar  $\text{Ph}_3\text{Si}\cdot$ ,<sup>24,27-33</sup> nonplanar  $\text{Ph}_3\text{Ge}\cdot$ ,<sup>24,33,37-41</sup> and nonplanar  $\text{Ph}_3\text{Sn}\cdot$ ,<sup>33,40,42-45</sup> radicals does suggest that two compensating effects operate along this series. That is, a progressive red shift as  $M$  changes from  $\text{C}$  through to  $\text{Sn}$ , which is clearly manifest in the  $(\text{alkyl})_3M\cdot$  series (see Figure 3), is masked by a compensating blue shift caused by reduced delocalization of the unpaired electron into the phenyl rings. The latter effect, which, in the  $\text{Ph}_3M\cdot$  radicals, arises from the combination of a nonplanar configuration for the triphenyl-heteroatom-centered radicals and the increasing size of the heteroatom, is clearly visible in the spectra of the carbon-centered series of radicals,  $\text{Ph}_3\text{C}\cdot$ ,  $\text{Ph}_2\text{CH}\cdot$ , and  $\text{Ph}\dot{\text{C}}\text{H}_2$  and of the silicon-centered series  $\text{Ph}_3\text{Si}\cdot$ ,  $\text{Ph}_2\text{SiH}\cdot$ , and  $\text{PhSiH}_2\cdot$  (see Figure 2).

**Registry No.**  $\text{PhCH}_3$ , 108-88-3;  $\text{Ph}_2\text{CH}_2$ , 101-81-5;  $\text{Ph}_3\text{CH}$ , 519-73-3;  $\text{Et}_3\text{SiH}$ , 617-86-7;  $\text{PhSiH}_3$ , 694-53-1;  $\text{Ph}_2\text{SiH}_2$ , 775-12-2;  $\text{Ph}_3\text{SiH}$ , 789-25-3;  $\text{Bu}_3\text{GeH}$ , 998-39-0;  $\text{Ph}_3\text{GeH}$ , 2816-43-5;  $\text{Bu}_3\text{SnH}$ , 688-73-3;  $\text{Ph}_3\text{SnH}$ , 892-20-6;  $\text{Me}_3\text{CO}\cdot$ , 3141-58-0;  $\text{Et}_3\text{Si}\cdot$ , 24669-77-0;  $\text{PhSiH}_2\cdot$ , 72975-30-5;  $\text{Ph}_2\text{SiH}\cdot$ , 73818-10-7;  $\text{Ph}_3\text{Si}\cdot$ , 18602-99-8;  $\text{Bu}_3\text{Ge}\cdot$ , 55321-84-1;  $\text{Bu}_3\text{Sn}\cdot$ , 20763-88-6;  $\text{Ph}_3\text{Sn}\cdot$ , 17272-58-1.

**Supplementary Material Available:** Tables II–XVII containing detailed kinetic information (15 pages). Ordering information is given on any current masthead page.

(35) Anderson, L. C. *J. Am. Chem. Soc.* **1935**, *57*, 1673–1676. Linschitz, H.; Berry, M. G. *Schweitzer, D. Ibid.* **1954**, *76*, 5833–5839.

(36) Scaiano, J. C. *J. Am. Chem. Soc.* **1980**, *102*, 5399–5400.

(37) Sakurai, H.; Mochida, K.; Kira, M. *J. Am. Chem. Soc.* **1975**, *97*, 929–931; *J. Organomet. Chem.* **1977**, *124*, 235–252.

(38) Geoffroy, M.; Givet, L.; Lucken, E. A. C. *Chem. Phys. Lett.* **1976**, *38*, 321–324.

(39) See also: Gynane, M. J. S.; Lappert, M. F.; Rivière, P.; Rivière-Baudet, M. *J. Organomet. Chem.* **1977**, *142*, C9–C11.

(40) Note that diarylalkylgermyl<sup>41</sup> and trialkyltin<sup>42</sup> radicals generated from chiral precursors react with  $\text{CCl}_4$  to give optically active products with retained stereochemistry.

(41) Sakurai, H.; Mochida, K. *Chem. Commun.* **1971**, 1581.

(42) Gielen, M.; Tondeur, Y. *Nouv. J. Chim.* **1978**, *2*, 117–118.

(43) Berclaz, T.; Geoffroy, M. *Chem. Phys. Lett.* **1977**, *52*, 606–610.

(44) King, B. A.; Bramwell, F. B. *J. Inorg. Nucl. Chem.* **1981**, *43*, 1479–1481.

(45) See also: Lehnig, M.; Buschhaus, H.-U.; Neumann, W. P.; Apoussidis, Th. *Bull. Soc. Chim. Belg.* **1980**, *89*, 907–914. Lehnig, M.; Dören, K. *J. Organomet. Chem.* **1981**, *210*, 331–341. Buschhaus, H.-U.; Neumann, W. P.; Apoussidis, Th. *Liebigs Ann. Chem.* **1981**, 1190–1197. El-Fanargy, A. F.; Lehnig, M.; Neumann, W. P. *Chem. Ber.* **1982**, *115*, 2783–2794.

(29) Sommer, L. H.; Ulland, L. A. *J. Org. Chem.* **1972**, *37*, 3878–3881.

(30) A study of the ESR spectrum of  $\text{Ph}_3\text{Si}\cdot$  trapped in a matrix gave  $a_{29\text{Si}} = 79.6$  G,<sup>31</sup> which value is considerably smaller than the value of 181 G found for  $\text{Me}_3\text{Si}\cdot$  in solution.<sup>32</sup> This indicates that the orbital containing the unpaired electron has much less s character in  $\text{Ph}_3\text{Si}\cdot$  than in  $\text{Me}_3\text{Si}\cdot$ , and this, in turn, that there is less bending at the radical center in the former radical. In the trimesitylsilyl radical  $a_{29\text{Si}}$  rises to 135 G<sup>33</sup> but in this case the steric effect of the ortho methyl groups probably causes a propeller like arrangement of the aromatic rings, which reduces electron delocalization and makes this silyl radical more similar in configuration to  $\text{Me}_3\text{Si}\cdot$  than to  $\text{Ph}_3\text{Si}\cdot$ .

(31) Geoffroy, M.; Lucken, E. A. C. *Helv. Chim. Acta* **1970**, *53*, 813–818.

(32) Krusic, P. J.; Kochi, J. K. *J. Am. Chem. Soc.* **1969**, *91*, 3938–3940.

(33) Gynane, M. J. S.; Lappert, M. F.; Riley, P. I.; Rivière, P.; Rivière-Baudet, M. *J. Organomet. Chem.* **1980**, *202*, 5–12.

(34) Parkes, D. A.; Quinn, C. P. *Chem. Phys. Lett.* **1975**, *33*, 483–490.